DOI 10.1515/htmp-2012-0079 — High Temp. Mater. Proc. 2012; 31(4-5): 439–449

Noriaki Kurita*, Kenji Kobayashi, Yoshinori Heda and Norihiko Fukatsu

Oxygen Liberation from Stabilized Zirconia upon Changing DC Polarization Condition

Abstract: The compositional change of stabilized zirconia upon the change of oxygen chemical potential was studied by applying DC-polarization method to a galvanic cell using stabilized zirconia as the electrolyte. The flow of excess charge observed upon the change of the DC-polarization condition was found due to the oxygen liberation from the bulk of the electrolyte. The total amount of liberated oxygen determined by the excess charge was analyzed in terms of the compositional change of the electrolyte due to the change of oxygen chemical potential profile in the electrolyte. The calculated values based on the increase or decrease of the electronic defects could not account for the experimental values. However, the ones based on the reduction of impurity oxides were in good agreement with the experimental values. Considerable amount of oxygen can be released from or absorbed into the zirconia electrolyte by the redox reaction of impurity oxide. It is noteworthy that this phenomenon may cause serious errors to the transport properties of electronic defect determined with the use of the relaxation processes.

Keywords: solid electrolyte, drift mobility of excess electron, non-stoichiometry, high temperature

PACS® (2010). 72.60.+g

***Corresponding author: Noriaki Kurita:** Department of Environment and Materials Engineering, Nagoya Institute of Thechnology, Gokiso-cho, Showa-ku, Nagoya 466-8555, Japan
E-mail: kurita@nitech.ac.jp
Kenji Kobayashi: Department of Environment and Materials Engineering, Nagoya Institute of Thechnology, Gokiso-cho, Showa-ku, Nagoya 466-8555, Japan
Yoshinori Heda: Department of Environment and Materials Engineering, Nagoya Institute of Thechnology, Gokiso-cho, Showa-ku, Nagoya 466-8555, Japan
Norihiko Fukatsu: Industrial Chemical Sensor Laboratory, Nagoya Institute of Technology, Crystal Plaza 4F, 3-101-1 Honmachi, Tajimi 507-0033, Japan, E-mail: fukatsu@nitech.ac.jp

1 Introduction

It has generally been considered that the composition of the stabilized zirconia is very stable and the amount of oxygen vacancies remains almost constant for the ordinary oxygen potential and temperature ranges within the "ionic domains". However, based on their highly sensitive measurements, Otsuka and Kozuka [1–3] observed a phenomenon which may be attributed to the liberation of oxygen from the electrolytes. If this is the case, it may affect the accuracy of some measurements using the zirconia electrolyte, for example, the determination of amounts of oxygen by a coulometry, the determination of dissolved oxygen in molten metals by consumable type sensors, etc. In order to estimate the extent of this effect, the phenomenon was investigated in more detail.

In this report, the amount of oxygen liberated from commercial stabilized zirconia used as the electrolyte of the galvanic cell was measured for various DC-polarization conditions and the results were analyzed by taking into account both the intrinsic and extrinsic mechanisms.

2 Theory

Consider the following cell,

$$\mathrm{Ar, Ag(l)|ZrO_2(+CaO)|Pt, Air\ (or\ CO_2/CO)}$$

the assembly of which is given schematically in Fig. 2. This type of cell is the same as that originally developed by Rapp and others [4] in order to determine the oxygen solubility and diffusivity in liquid metals. The left electrode is liquid silver melted in a closed chamber filled with pure Ar and the right electrode is a porous platinum electrode equilibrated with flowing air or a CO_2/CO gas mixture. The oxygen potential of the left electrode is determined by the amount of oxygen dissolved in the liquid silver. This electrode is closed and then works irreversibly when the cell is set under DC polarization conditions. On the contrary, the

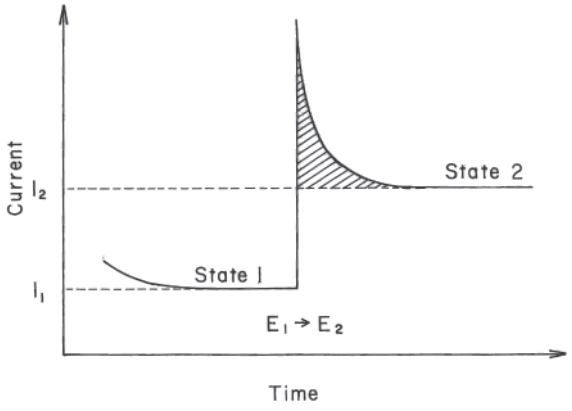

Fig. 1: Schematic view of the variation of the current upon the change of the polarization conditions.

oxygen potential of the right electrode is kept constant with flowing air or a CO_2/CO gas mixture. In this case, this electrode remains reversible when the cell is polarized. We call this electrode as the reference electrode.

When a voltage E_1 is applied to this cell so as to keep the left electrode negative, a current is seen to flow through the cell, and after some time, the Hebb-Wagner polarization condition [5] is attained and a steady electronic current I_1 is obtained as schematically shown in Fig. 1. We call this stable state "state 1". The applied voltage is suddenly changed to the new value E_2, so as to decrease the oxygen content of the liquid silver by electrolysis. A large current occurs through the cell and finally the next steady-state current I_2 will be attained. We call this state "state 2". As the change in electronic current during the electrolysis is thought to be small, the charge Q owing to the ionic current may be obtained by integration of the total current relaxation curve, after correcting for a constant electronic current (hatched area in Fig. 1). Q may be represented as,

$$Q = Q_{Ag} + Q_{ZrO_2} \tag{1}$$

where Q_{Ag} is the charge owing to the oxide ion current due to the oxygen drown out from the Ag electrode and Q_{ZrO_2} is the charge due to the compositional change of the electrolyte itself.

Q_{Ag} can be evaluated precisely from the thermodynamic data for the solubility of oxygen in liquid silver. At the Hebb-Wagner polarization condition, the oxygen concentration in the silver electrode is considered to be uniform. The oxygen partial pressures in equilibrium with the silver electrode, $(p_{O_2})_1$ and $(p_{O_2})_2$ for the respective applied voltages E_1 and E_2 can be calculated as follows,

$$(p_{O_2})_1 = (p_{O_2})_r \exp\left(\frac{4FE_1}{RT}\right) \tag{2}$$

$$(p_{O_2})_2 = (p_{O_2})_r \exp\left(\frac{4FE_2}{RT}\right) \tag{3}$$

where $(p_{O_2})_r$ is the oxygen partial pressure at the reference electrode, F is Faraday's constant, R is the gas constant, and any polarization effect at the Ag electrode is neglected. Hence, the concentrations of oxygen for the silver electrode in mole fraction c_1 and c_2 in the respective states 1 and 2 may be represented as,

$$c_1 = \left(\frac{1}{\gamma_O}\right)\left(\frac{(p_{O_2})_1}{p^{\varnothing}_{O_2}}\right)^{1/2} \tag{4}$$

$$c_2 = \left(\frac{1}{\gamma_O}\right)\left(\frac{(p_{O_2})_2}{p^{\varnothing}_{O_2}}\right)^{1/2} \tag{5}$$

where γ_O is the activity coefficient of oxygen in liquid Ag and $p^{\varnothing}_{O_2}$ is the pressure of the standard state of pure oxygen. The value M_O, the amount of oxygen drown out from the silver electrode for the change of state 1 to state 2, may be calculated as follows,

$$M_O = \left(\frac{M_{Ag}}{\gamma_O}\right)\left[\left(\frac{(p_{O_2})_1}{p^{\varnothing}_{O_2}}\right)^{1/2} - \left(\frac{(p_{O_2})_2}{p^{\varnothing}_{O_2}}\right)^{1/2}\right] \tag{6}$$

where M_{Ag} is the gm moles of the Ag electrode. This oxygen can be considered to have been transferred by the flow of oxide ions through the electrolyte and released at the reference electrode. Therefore, by using the equation (2), (3) and (6), Q_{Ag} is represented by,

$$Q_{Ag} = \left(\frac{M_{Ag}}{\gamma_O}\right)\left(\frac{(p_{O_2})_r}{p^{\varnothing}_{O_2}}\right)^{1/2}\left[\exp\left(\frac{2FE_1}{RT}\right) - \exp\left(\frac{2FE_2}{RT}\right)\right] \tag{7}$$

Therefore, Q_{ZrO_2}, the charge due to the compositional change of the electrolyte itself, may be calculated by subtracting the value Q_{Ag} from Q, which is experimentally obtained from the total current relaxation curve.

3 Experimental

The apparatus used in the present work was approximately the same as that used by Otuka and Kozuka [3]. The schematic view of the assembly is shown in Fig. 2. Calcia-stabilized zirconia tubes were used as the electrolytes. They were supplied by Nikkato Corp. with dimensions of 8 mm o. d. and 5 mm i. d. and 300 mm long. Two sorts of zirconia tubes of different purity were used.

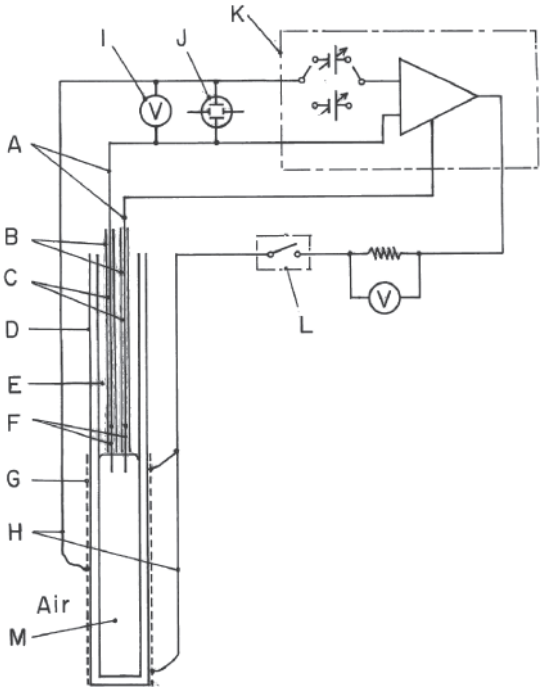

Fig. 2: Schematic diagram of the cell assembly. A: Kanthal lead wires, B: Alumina sheath, C: Stabilized zirconia crucible as a sample, E: Argon gas, F: Iridium wires, G: Porous platinum electrode, H: Platinum lead wires, I: Voltmeter, J: Oscilloscope, K: Potentiostat, L: Interrupter, M: Liquid silver electrode.

Species	Composition (mass%)	
	Type A	Type B
SiO_2	0.14	1.02
TiO_2	0.08	0.11
Al_2O_3	0.68	0.52
Fe_2O_3	0.05	0.15
MgO	tr.	0.15
Na_2O	0.01	0.03
CaO	5.86	6.01
ZrO_2	93.18	92.01

Table 1: Composition of the samples.

Type A was high purity grade and Type B was low purity grade; the compositions of these samples are shown in Table 1.

On the surface of the zirconia tubes over a 6 cm length from the closed end, a porous platinum layer for reference electrode was prepared by painting platinum paste and sintering in air for 5 hr at 1273 K. 99.999% pure silver was used as the inner electrode. The depth of the molten silber was set the same as the length of the outer electrode. Over the silver electrode, purified Ar was filled and the electrode was sealed during the experiment. A platinum lead wire was connected to the outer electrode. Kanthal wire was used as the lead wire to the inner electrode. A short length of iridium wire welded to the end of the Kanthal wire were used to contact with the liquid silver. Thermal electromotive force between the two lead wires was measured beforehand and the applied voltage was corrected according to the data.

A specially designed potentiostat was used to provide a sudden change in the applied voltage on the cell. The schematic electrical circuit to the cell is shown in Fig. 2. By using the potentiostat, the IR drop in the lead wire may be eliminated and the applied voltage can be changed suddenly to the preselected value. The voltage drop, due to the electrode resistanse, cannot be eliminated from this procedure. This correction was made by evaluating the resistance of the electrode measuring the voltage drop in the oscilloscope upon the interruption of the current. The values of applied voltage reported here are the values corrected for the thermoelectric voltage and for the electrode effect.

A Nicrome-wound furnace and an electronic controller were used to maintain the temperature of the cell within ±2 K at 1273, 1373 and 1473 K.

4 Results

4.1 Identification of the carrier of the excess charge flow

In Fig. 3, typical examples of the current decay curve measured upon changing the applied voltage are shown for two distinct polarization conditions. In both cases, the applied voltage was changed by 100 mV more negative than the initial values. Case A is for moderately reduced conditions, where the oxygen concentration in liquid Ag is relatively large, and the main part of the observed current should be due to the change in oxygen dissolved in the liquid Ag electrode. On the contrary, case B is the condition of a highly reduced state. The oxygen chemical potential at the liquid Ag electrode is extremely low and, according to the evaluation from the thermodynamic data, the change in oxygen concentration should not be observed perfectly. But, as shown in the figure, small amounts of charge flow were observed upon changing the applied voltage. The charge corresponding to the hatched area, which we call "excess charge" in this text, is considered Q_{ZrO_2}, defined by the Eq. 1. The fact that this excess charge was due to the release of oxygen was also confirmed by observing that some amounts of oxygen were generating

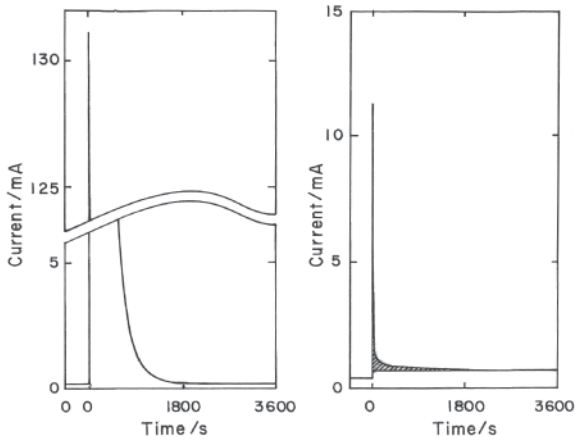

Fig. 3: Typical examples of the current decay after the changes of polarization conditions. Left Case A: For the change $E_{apply} = -140$ mV to $E_{apply} = -240$ mV. Right Case B: For the change $E_{apply} = -1000$ mV to $E_{apply} = -1100$ mV. Sample of Type A was used. The oxygen partial pressure of the reference electrode was kept at 0.21 atm. Measuring temperature was 1273 K.

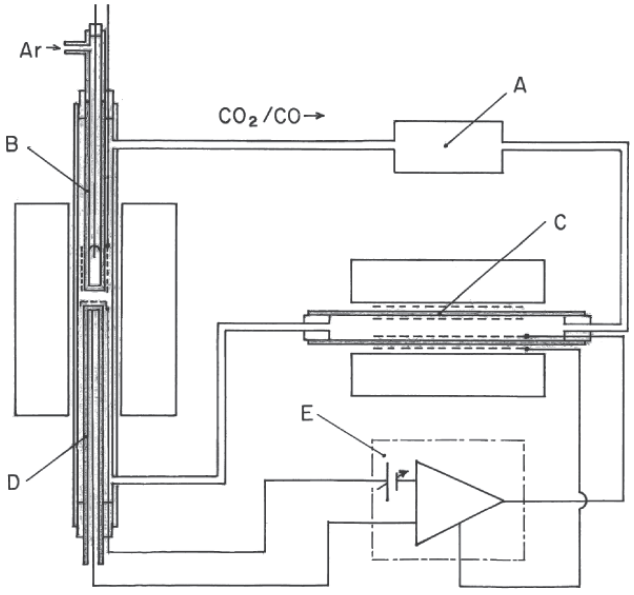

Fig. 4: Schematic diagram of the apparatus for the confirmation of the liberation of oxygen from the electrolyte sample upon the change of the polarization conditions. A: Circulation pump, B: Polarization cell, C: Oxygen pump, D: Oxygen sensor, E: Potentiostat.

simultaneously from the outer electrode, which is shown in the following measurement.

The apparatus used in this confirmation is shown in Fig. 4. The polarizing cell was contained in a chamber filled with a circulating CO_2/CO gas mixture. The ratio of the gas mixture was kept constant by the feedback control

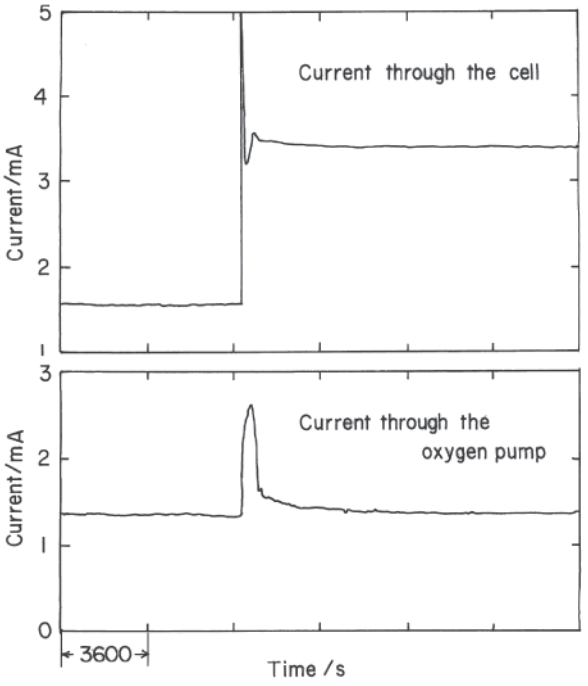

Fig. 5: Changes of the current through the cell and oxygen pump upon the change of cell polarization condition from $P_{O_2}/\text{atm} = 1.9 \times 10^{-16}$ to $P_{O_2}/\text{atm} = 4.9 \times 10^{-18}$. Upper: Change of the current through the cell. Lower: Change of the current through the oxygen pump. Sample of Type A was used. Oxygen partial pressure controlled at the reference electrode was 3.16×10^{-6} atm.

system using an oxygen sensor and an oxygen pump based on a stabilized zirconia solid electrolyte [6]. When oxygen is generated into the circulating gas compartment, the control system pumps it out by electrolysis to keep the oxygen potential of the circulating gas at the pre-selected constant value. Therefore, oxygen generation may be detected by monitoring the current through the oxygen pump.

The result is shown in Fig. 5. The cell was polarized from the state of the oxygen partial pressure in the liquid electrode of 1.9×10^{-16} atm to the state of 4.9×10^{-18} atm. For these conditions, the change in oxygen concentration in the liquid Ag electrode is thoroughly negligible. The upper figure shows the variation of the current through the sample cell upon the polarization. The lower figure shows the current variation through the oxygen pump. As the figure shows, some oxygen is released from the cell even in these highly reduced polarization conditions. Unfortunately, quantitative analysis could not be possible since the composition of the circulating gas was selected at such an extreme ratio and the oxygen potential of this reference electrode is not so stable as air or a buffered gas mixture. Therefore, long term integration of the current could not be possible. But almost all of the net charge flow

observed in the polarization cell may be considered to be the flux of oxygen ions.

4.2 Relation between the applied voltage and the amounts of the charge flow

The accumulative amount of charge generated upon the change of the polarization condition at 1273 K is plotted as a function of the final applied voltage in Fig. 6. The arbitrary starting condition was selected at the applied voltage of –500 mV with respect to the air reference electrode, whose state is corresponding to the equilibrium oxygen pressure of 2.5×10^{-9} atm. The plots fall on a unique curve, regardless of the difference of the increments of the applied voltage and the different cells assembled with the electrolyte of the same lot. The broken line represents the thermodynamically calculated amounts of charge due to the oxygen drown out from the liquid silver electrode, Q_{Ag}. The excess charge, Q_{ZrO_2}, may be determined by subtracting Q_{Ag} from the total charge. From these data, it was concluded that the value Q_{ZrO_2} is determined uniquely by the initial and final polarization conditions. This evidence suggests that this amount of excess charge results from some changes in the bulk constitution of the electrolyte.

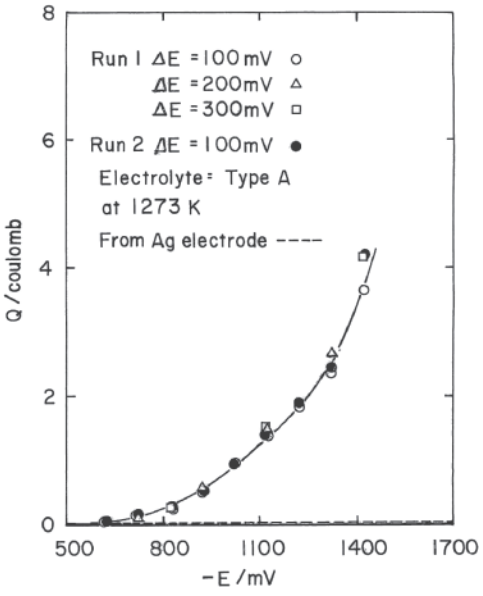

Fig. 6: Accumulated amounts of the excess charge for the different increment of the polarization voltage.

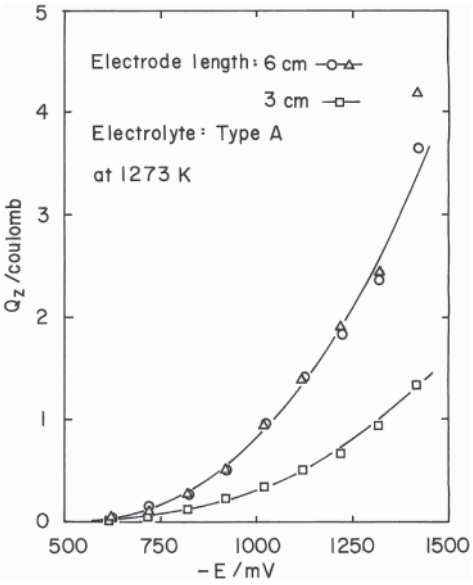

Fig. 7: The effect of the dimension of the electrode on the accumulated amounts of the excess charge.

4.3 Relation between the amount of excess charge and the dimensions of the electrolyte

The effect of the electrolyte dimensions to the amount of the excess charge is shown in Fig. 7. When electrolyte tubes of the same diameter were used, the excess charge was nearly proportional to the length of the electrode. If the excess charge resulted from oxygen flow from the gas phase over the liquid inner electrode, it would be independent from the length of the electrode. This evidence also supports the assumption that the excess charge results from some changes in the bulk constitution of the electrolyte.

4.4 Relation between the amount of excess charge and that of the impurities of the electrolyte

The effect of the amount of the impurities of the electrolyte on the amount of the excess charge was studied by measuring two different types of the electrolyte of the same geometry. The results are given in Fig. 8. The difference between measured values on the same lot of electrolyte could be ignored. But the difference between the electrolytes with different amounts of impurities was very large. The measured excess charge was larger for less pure specimen than for that of high purity.

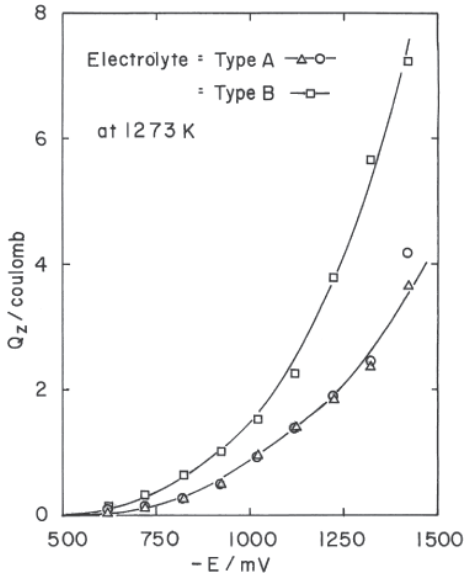

Fig. 8: The effect of the amounts of impurity of the sample on the accumulated excess charge.

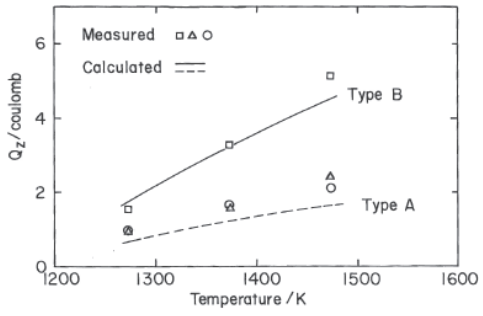

Fig. 9: The effect of temperature on the amounts of the excess charge generated from the stable condition $E_{apply} = -500$ mV to $E_{apply} = -1000$ mV. Lines are calculated values based on the model of oxygen liberation due to the reduction of the impurity oxides.

4.5 Relation between the amount of excess charge and the measuring temperature

The effect of the measuring temperature on the amount of the excess charge observed upon a change of the polarization conditions from E_1: –500 mV to E_2: –1200 mV (with respect to the air reference electrode), is shown in Fig. 9 as a function of the temperature. The measured extra charge is observed to increase with increasing temperature. This trend is similar for both different impurity types of electrolytes. At 1473 K, the steady ion blocking state was not obtained at a highly polarized conditions; the polarizing current increased gradually. This phenomenon results from an irreversible compositional change in the electrolyte, and the data obtained for these conditions were discarded.

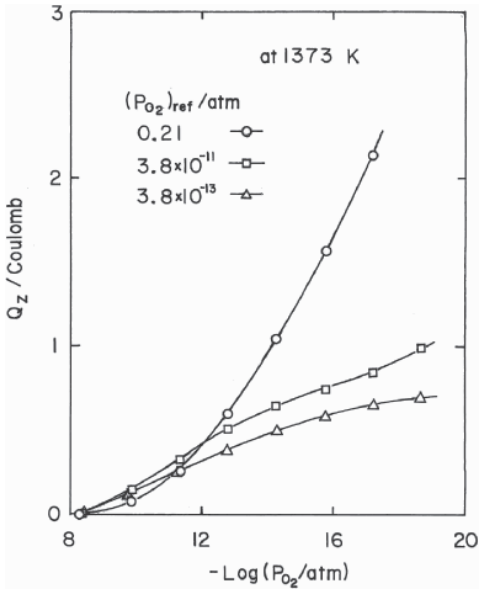

Fig. 10: The effect of the oxygen potential of the reference electrode on the accumulated excess charge. Sample of Type A was used.

4.6 Relation between the amount of the excess charge and the oxygen potential of the reversible electrode

The polarization experiments performed while keeping the oxygen potential of the reversible electrode at low values with CO_2/CO gas mixtures are summarized in Fig. 10. The measured amount of excess charge for each experiment is a function of the oxygen potential of the irreversible electrode. An arbitrary starting point was selected at P_{O_2}: 3.16×10^{-8} atm. As shown in Fig. 10, the amount of charge for the reduced electrode is larger than that for the air electrode up to about $\log(P_{O_2}/\text{atm}) = -13$. But in the higher polarized state this relation is reversed.

5 Discussion

The above results show that the observed flow of excess charge can be attributed to the transport of ionic oxygen generated from a constitutional change in the electrolyte upon a variation in the potential profile in the electrolyte. Some quantitative discussions on these results are given in the follows.

The potential profile established in the electrolyte at the polarized state may be calculated according to the theory of Choudhury and Patterson [7]. The relation between the oxygen potential and the normalized distance from the end of the electrolyte x/L is given as follows,

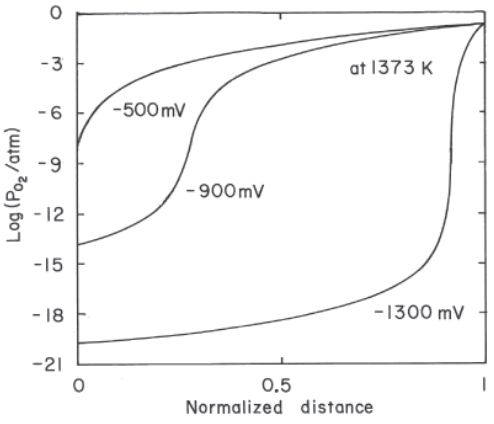

Fig. 11: The calculated potential profiles established in the polarized sample for some different polarization conditions.

$$x/L = \frac{\ln(P_{O_2}/P'_{O_2}) - \int_{P'_{O_2}}^{P_{O_2}} t_{ion}\, d(\ln P_{O_2})}{\ln(P''_{O_2}/P'_{O_2}) - \int_{P'_{O_2}}^{P''_{O_2}} t_{ion}\, d(\ln P_{O_2})} \tag{8}$$

where L is the thickness of the electrolyte, P_{O_2}, P'_{O_2} and P''_{O_2} are the oxygen pressures at $x = x$, $x = 0$ and $x = L$, respectively. Examples of potential profile which would be established in the electrolyte for some different polarization conditions were calculated and are shown in Fig. 11. The values of the electrical properties of electrolyte used in the calculations are shown in Table 2, which were measured values to the present electrolyte samples [8]. Two mechanisms of the generation of oxygen upon such a change in potential profiles are considered as follows.

5.1 Variation of concentration of oxygen vacancy due to intrinsic mechanism

The oxygen vacancies in the stabilized zirconia are considered to be in the local equilibrium with surrounding oxygen gas and electronic imperfections [9]. These are expressed by the reactions,

$$O_O^{\times} = V_O^{\bullet\bullet} + 2e' + \frac{1}{2}O_2 \tag{9}$$

$$O_O^{\times} + 2h^{\bullet} = \frac{1}{2}O_2 + V_O^{\bullet\bullet} \tag{10}$$

When the equilibrium of these reactions shifts to the right by decreasing the oxygen potential, oxygen may be generated leaving vacancies. These quantities are calculated here.

The concentrations of excess electrons C_e and positive holes C_h are buffered by the large amount of normal oxide ions and oxide ion vacancies as shown by the equilibrium reaction equations (9) and (10), and may be expressed as follows,

$$C_e = KP_{O_2}^{-1/4}, \quad C_h = K'P_{O_2}^{1/4} \tag{11}$$

From the relation between the conductivity and the charge-carrier concentration,

$$C_e = \frac{\sigma_{ion}}{Fu_e}\left(\frac{P_{O_2}}{P_{\ominus}}\right)^{-1/4} \tag{12}$$

$$C_h = \frac{\sigma_{ion}}{Fu_h}\left(\frac{P_{O_2}}{P_{\oplus}}\right)^{1/4} \tag{13}$$

where u_e and u_h are the mobility of the excess electron and positive hole respectively, and $P_{\ominus}$ and $P_{\oplus}$ represent the oxygen partial pressures at which the partial conductivities of excess electron and the positive hole becomes the same value as that of oxygen ion, σ_{ion}, respectively [10]. Then the concentration profiles of excess electrons and positive holes are established in the bulk of the electrolyte. Equation (9) shows that the increase of two moles of excess electrons leads to the increment of one mole of oxygen vacancies and one mole of oxygen atom generation. On the other hand, Equation (10) means that the decrease

Samples	Temperature/K	σ_{ion}/S cm^{-1}	log($P_{\ominus}$/atm)	log($P_{\oplus}$/atm)
Type A	1273	0.015	−28.1	9.0
	1373	0.045	−25.7	9.4
	1473	0.117	−23.5	9.8
Type B	1273	0.014	−28.4	9.0
	1373	0.037	−25.7	9.1
	1473	0.084	−23.4	9.2

Table 2: Electrical properties of the samples.

of two moles of electron holes introduces one mole of oxygen vacancies and one mole of oxygen atom generation. Therefore, the amount of excess oxygen to be released when the oxygen potential profile was changed, Δn_O, is represented by,

$$\Delta n_O = \frac{AL\sigma_{ion}}{2F}\left[\frac{U_2 - U_1}{u_e} + \frac{U_3 - U_4}{u_h}\right] \tag{15}$$

where A is the cross-sectional area of the electrolyte and U_1 to U_4 are,

$$\begin{aligned} U_1 &= \int_0^1 \left(\frac{P'_{O_2}}{P_\ominus}\right)^{-1/4} d\left(\frac{x}{L}\right) \\ U_2 &= \int_0^1 \left(\frac{P''_{O_2}}{P_\ominus}\right)^{-1/4} d\left(\frac{x}{L}\right) \\ U_3 &= \int_0^1 \left(\frac{P'_{O_2}}{P_\oplus}\right)^{1/4} d\left(\frac{x}{L}\right) \\ U_4 &= \int_0^1 \left(\frac{P''_{O_2}}{P_\oplus}\right)^{1/4} d\left(\frac{x}{L}\right) \end{aligned} \tag{16}$$

At the reference electrode, according to the electrode reaction,

$$O_O^\times(\text{electrolyte}) = V_O^{\bullet\bullet}(\text{electrolyte}) + 2e(\text{electrode}) + \frac{1}{2}O_2(\text{gas}) \tag{17}$$

the excess oxygen conveyed as the oxide ion is released from the electrolyte. On the other hand, across the interface of the irreversible electrode, the electricity is charged by the pair of electron and accumulated oxide ion vacancy. This flow of oxide ion gives the excess current in the external circuit. The amount of the electric charge $_{ZrO}$, then, may be represented as,

$$Q_{ZrO_2} = 2F\Delta n_O \tag{18}$$

The integral terms in the Eq. (16) can be numerically calculated from the potential profile represented by the Eq. (8). To perform the calculation, the values of the mobility of excess electron and positive hole for zirconia are necessary. The reported values, however, are inconsistent. In the present calculation, the mobility was assumed to be 0.8 $cm^2V^{-1}s^{-1}$ for both excess electron and positive hole [11]. This value is the representative value of the data obtained by the thermo-electric power measurement, for which the effect of impurity of the sample is thought to be small. In the calculation, the electrolyte was taken as the plane sheet because the thickness was small compared to its diameter.

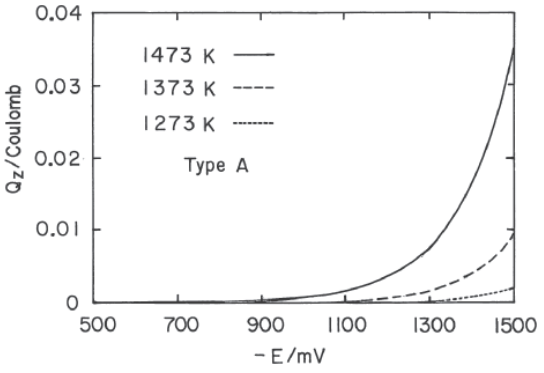

Fig. 12: The calculated amounts of excess charge based on the model of the intrinsic mechanism.

The results are shown in Fig. 12. The calculated values are only about 1/1000 – 1/10000 of the measured values and do not account for the observed large flow of excess charge. If the more small values obtained by the potential relaxation measurement [12] were adopted, the better agreement might be obtained. But the experimental fact that this excess charge is also depending on the amount of impurity could not be explained. Because a small difference of impurity scarcely affects the potential profile in the electrolyte and the concentration profile of excess electron and positive hole does not change largely.

5.2 Generation of oxygen due to the reduction of the oxide impurities

Among the impurities in the electrolyte shown in Table 1, Fe and Ti should be noted because their valency may vary with oxygen potential. From EPMA analysis, Ti was fully dissolved into matrix of the electrolyte. A part of the Fe was observed to concentrate in a second phase between the grains. However, since the estimation of its composition is difficult, Fe and Ti are taken to exist as fully dissolved components in the electrolyte here. Clearly, this assumption can only lead to a higher value for concentration of these impurity ions.

Fe and Ti on zirconium sites may be considered to be involved in the equilibria,

$$2Fe'_{Zr} + O_O^\times = 2Fe''_{Zr} + V_O^{\bullet\bullet} + \frac{1}{2}O_2 \tag{19}$$

$$2Ti_{Zr}^\times + O_O^\times = 2Ti'_{Zr} + V_O^{\bullet\bullet} + \frac{1}{2}O_2 \tag{20}$$

where Fe'_{Zr} denotes trivalent Fe, Fe''_{Zr} divalent Fe, Ti^{x}_{Zr} tetravalent Ti and Ti'_{Zr} trivalent Ti situated at a zirconium site. The oxygen may be released when the above equilibrium reactions shift to the right according to the change of the oxygen profile. In the following analysis, the amount of oxygen released with the ferrous/ferric redox reaction is only shown as an example.

Equation (19) may be expressed by the molecular components as follows,

$$\underline{FeO_{1.5}} = \underline{FeO} + \frac{1}{4}O_2 \tag{21}$$

where the underlined components denote that those are dissolved in the stabilized zirconia.

From above relation,

$$\frac{\gamma_{FeO_{1.5}} N_{FeO_{1.5}}}{\gamma_{FeO} N_{FeO} P_{O_2}^{1/4}} = K \tag{22}$$

where K is the equilibrium constant of the reaction (21), γ_{FeO} and $\gamma_{FeO_{1.5}}$ are the activity coefficients and N_{FeO} and $N_{FeO_{1.5}}$ are the mole fraction of FeO and $FeO_{1.5}$, respectively. As the total mass of Fe is constant,

$$N_{FeO} + N_{FeO_{1.5}} = N_{Fe} \tag{23}$$

where N_{Fe} denotes mole fraction of total Fe. Solving Equations (22) and (23) simultaneously,

$$N_{FeO_{1.5}} = \frac{N_{Fe} P_{O_2}^{1/4}}{\frac{\gamma_{FeO_{1.5}}}{\gamma_{FeO}} K + P_{O_2}^{1/4}} \tag{24}$$

Similarly, for titanium,

$$N_{TiO_2} = \frac{N_{Ti} P_{O_2}^{1/4}}{\frac{\gamma_{TiO_2}}{\gamma_{TiO_{1.5}}} K' + P_{O_2}^{1/4}} \tag{25}$$

where N_{Ti} is the mole fraction of total Ti, γ_{TiO_2} and $\gamma_{TiO_{1.5}}$ the activity coefficients of TiO_2 and $TiO_{1.5}$ dissolved in the stabilized zirconia, and K' is the equilibrium costant for the reaction,

$$TiO_2 = TiO_{1.5} + \frac{1}{4}O_2 \tag{26}$$

When the polarization condition was changed and the profile for the distribution of $FeO_{1.5}$ varies from $N'_{FeO_{1.5}}\left(\frac{x}{L}\right)$ to $N''_{FeO_{1.5}}\left(\frac{x}{L}\right)$ and the distribution of TiO_2 varies from $N'_{TiO_2}\left(\frac{x}{L}\right)$ to $N''_{TiO_2}\left(\frac{x}{L}\right)$, respectively, the amount of the liberated oxygen Δn_O may be represented as,

$$\Delta n_O = \frac{1}{2} n_{ZrO_2} \left[\int_0^1 N'_{FeO_{1.5}}\, d\left(\frac{x}{L}\right) - \int_0^1 N''_{FeO_{1.5}}\, d\left(\frac{x}{L}\right) \right] + \frac{1}{2} n_{ZrO_2} \left[\int_0^1 N'_{TiO_2}\, d\left(\frac{x}{L}\right) - \int_0^1 N''_{TiO_2}\, d\left(\frac{x}{L}\right) \right] \tag{27}$$

where, n_{ZrO_2} is total moles of the electrolyte.

If this oxygen is released from the reference electrode, the observed excess charge Q_{ZrO_2} is,

$$Q_{ZrO_2} = 2F\Delta n_O \tag{28}$$

The amount of excess charge was calculated according to this model for the present experimental conditions. In the calculation, the equilibrium constant K and K' in Equations (24) and (25) were taken from the tabulated data of Barin et al [13]. The activities of these oxides are not known, but it is reasonable to assume that the activities of FeO (or $TiO_{1.5}$) and $FeO_{1.5}$ (or TiO_2) is not largely different from each other. This assumption leads to the relations

$$\frac{\gamma_{FeO_{1.5}}}{\gamma_{FeO}} = 1, \quad \frac{\gamma_{TiO_2}}{\gamma_{TiO_{1.5}}} = 1. \tag{29}$$

The calculated results are shown in Fig. 13. The values are several times larger than those observed, but dependency on the oxygen potential of the irreversible electrode is quite good. These trends were also observed for electrolyte which contain a higher level of impurities.

The modification of constant K's and γ's were tried in order to fit the calculated value to the measured one, but good results were not obtained. On the contrary, when it was calculated supporting that only a part of the impurities participated in this mechanism, a fairly good agreement was possible. This fact may suggest that a part of the impurities is condensed in the silicate glassy phase located between the grain boundaries and does not take part in the oxygen liberation mechanism because the mobility of oxygen ions in these phase is very low [14]. On this point, more studies are needed. If about a half of the iron oxide is only reduced in valence, the excess charge may be calculated as in Fig. 14. These values are in good

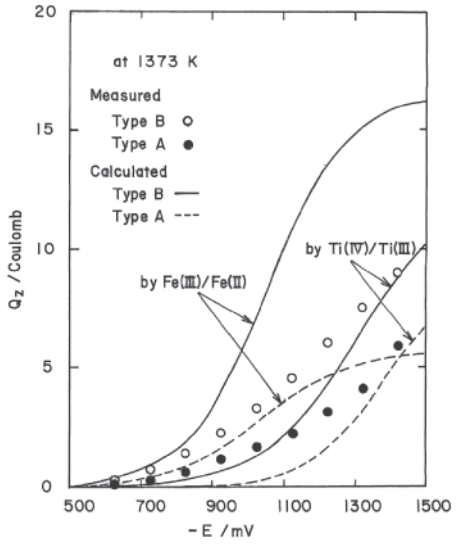

Fig. 13: The calculated amounts of excess charge based on the model of oxygen liberation due to the reduction of the impurity oxides.

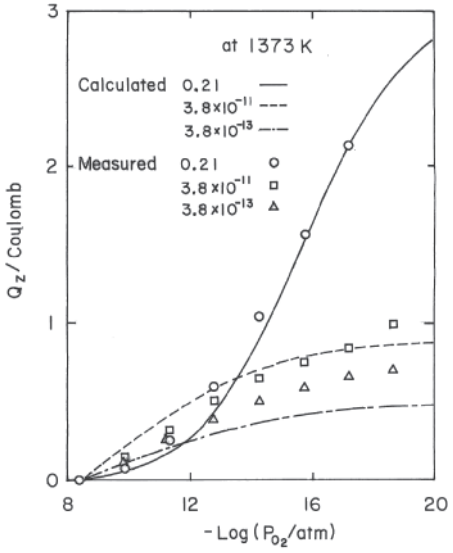

Fig. 14: The comparison between the measured excess charge and those estimated based on the model of the reduction of Fe_2O_3 for some experimental conditions with the different oxygen partial pressure of the reference electrode.

accordance with the observation not only for the different applied potentials but also for the different oxygen potentials of the reference electrodes. Furthermore, the calculated temperature dependence of the excess charge flow is also in fairly good agreement with the observed ones, as is seen in Fig. 9.

From these facts, it is concluded that the observed excess charge should be attributed to the flow of oxygen ion caused from the reduction of the dissolved impurity components in the electrolyte. This effect may affect the measurement of small quantity of oxygen with the use of coulometric method based on the solid electrochemical cell using stabilized zirconia as the electrolyte. Moreover, this effect may lead to very small values of the drift mobility of the excess electron and positive hole when they are determined from the conductivity and the carrier concentration measured by non-stoichiometry. The determination from the analysis of the relaxation process should also be affected by this effect. The relatively small values of drift mobility of electronic defects for stabilized zirconia reported so far should be reconsidered with the present effect in mind.

6 Conclusion

The mechanism of the flow of excess charge observed in the DC polarization of the zirconia solid electrolyte cell was investigated in detail. It was found reasonable to attribute the excess charge to the oxygen liberation resulting from the reduction of impurity components upon the change of the oxygen potential profile in the electrolyte. The oxygen liberation from the electrolyte should be considered when using the same materials under very low oxygen potential conditions.

Acknowledgements

The authors would like to thank Mr. M. Ichimura, Mr. H. Tanaka, Mr. H. Ohya and Mr. K. Hayakawa for their helps in the experiments.

Received: April 30, 2012. Accepted: July 11, 2012.

References

[1] S. Otsuka and Z. Kozuka, *Metall. Trans. B*, **10B**, 565–574 (1979).
[2] S. Otsuka, T. Sano and Z. Kozuka, *Metall. Trans. B*, **11B**, 313–319 (1980).
[3] S. Otsuka, Y. Matsumura and Z. Kozuka, *Solid State Ionics*, **3/4**, 495–498 (1981).
[4] K. E. Oberg, L. M. Friedman, W. M. Boorstein and R. A. Rapp, *Metall. Trans.*, **4**, 61–74 (1973).
[5] C. Wagner, *Z. Electrochem.*, **60**, 4–7 (1956).
[6] N. Fukatsu, I. Osawa and Z. Kozuka, *Trans. Japan Inst. Metal*, **19**, 25–34 (1978).
[7] N. S. Choudhury and J. W. Patterson, *J. Electrochem. Soc.*, **117**, 1384–1388 (1970).

[8] N. Fukatsu and N. Kurita, *to be published*.
[9] J. W. Patterson, E. C. Borgen and R. A. Rapp, *J. Electrochem. Soc*., **114**, 752–758 (1967).
[10] H. Schmalzried, *Ber. Bunsenges. Phys. Chem*, **66**, 572–576 (1962).
[11] J. W. Wimmer and I. Bransky, *"Electrical Conductivity in Ceramics and Glass", Part A*, Edited by N. M. Tallan, Dekker, New York (1974), pp. 304.
[12] W. Weppner, *J. Solid State Chem.*, **20**, 305–314 (1977).
[13] I. Barin and O. Knache, *"Thermochemical Properties of Inorganic Substances"*, Springer-Verlag, New York (1973).
[14] L. Heyne and D. D. Engelsen, *J. Electrochem. Soc.*, **124**, 727–735 (1977).